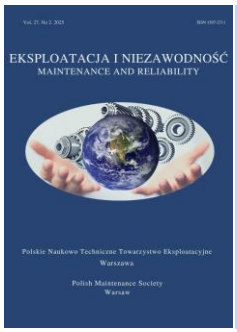

Eksploatacja i Niezawodnosc – Maintenance and Reliability

Volume 27 (2025), Issue 2

journal homepage: http://www.ein.org.pl

Article citation info:
Chen W, Hao S, Opportunistic maintenance for a novel load-sharing system with dependent degradation rate and volatility, Eksploatacja i Niezawodnosc – Maintenance and Reliability 2025: 27(2) http://doi.org/10.17531/ein/194165

Opportunistic maintenance for a novel load-sharing system with dependent degradation rate and volatility

Indexed by: Web of Science Group

Wei Chen[a], Songhua Hao[a,*]

[a] Sichuan University, China

Highlights

- A novel load-sharing system is presented with dependent degradation rate and volatility.
- System reliability is derived with general degradation rate-volatility-load correlation.
- OM strategy is introduced for the novel load-sharing system with economic dependence.

Abstract

For traditional degrading load-sharing systems, a typical assumption lies in the only effect of unit load on its degradation rate. However, motivated by a laser system example with positive correlation between degradation rate and volatility, we present a novel load-sharing system with general degradation rate-volatility-load correlation. Furthermore, to take account for unit economic dependence caused by sharable maintenance set-up cost, and the window period generated by the maintenance on some unit, opportunistic maintenance (OM) strategy is introduced to offer the opportunity of simultaneously maintaining another working unit under control-limit criteria. Based on the semi-regenerative process, the long-run average cost rate is minimized to obtain the optimal inspection interval, preventive maintenance and OM thresholds. Compared to the traditional condition-based maintenance strategy for each unit, the effectiveness of OM strategy is validated through numerical examples and case studies, offering broad managerial insights for engineers to reduce maintenance expenses.

Keywords
opportunistic maintenance, load-sharing system, dependent degradation rate and volatility, semi-regenerative process.

1. Introduction

A load-sharing system is a distinct form of redundancy comprising stochastically dependent components to collectively bear the entire system load [1], and has been widely applied across various engineering practices, including compressor stations [2], wind turbine generators [3] and hybrid power supply systems [4]. Within a traditional load-sharing system, the constituent units usually degrade over time, and only the degradation rates are affected by the sharing load [5]. In other words, the more load allocated to a unit, the faster its degradation process will be. Meanwhile, when any unit fails midway through the degradation process, its load will be redistributed to the remaining operational units, further hastening their degradation process and affecting the system remaining useful life [6].

Research for reliability modelling of degrading load-sharing systems has attracted widespread attention in recent years, especially based on discrete and monotone continuous unit degradation models. For example, Wu and Cui conducted reliability analysis for load-sharing k-out-of-n: G systems based on continuous-time Markov chains for interactive multi-state

(*) Corresponding author.
E-mail addresses: W. Chen (ORCID: 0009-0003-2931-5153) weic@stu.scu.edu.cn, S. Hao (ORCID: 0000-0001-6875-4800) haosonghua@scu.edu.cn,

subsystems [7]. Assuming the component degradation process follows an inverse Gaussian process, Ye et al. investigated the time-to-degradation-failure distribution for load-sharing systems [8]. In addition, few scholars focused on the non-monotonic continuous degradation model of load-sharing systems. Building upon unit degradation models with the Wiener process, Xu et al. proposed a model parameter estimation method for load-sharing systems [9]. Utilizing the log-linear link function to relate the degradation rates to load, Zhao et al. provided a reliability modeling framework for load-sharing systems based on step-wise drifted Wiener process [10].

As far as we are concerned, most existing studies of degrading load-sharing systems assume that the load a unit bears only has an influence on its degradation rate (drift parameter), with its degradation volatility (diffusion parameter) unaffected. However, a positive correlation between degradation rate and volatility is commonly observed for many practical products, such as aluminum alloy [11] and GaAs lasers [12]. In other words, when the degradation rate of such a product is accelerated, its degradation volatility also increases [13]. Under this circumstance, for load-sharing systems consisting of such products, e.g., a laser system with more than one GaAs laser and specific system-level output power requirements, the unit load will have effects on both its degradation rate and volatility. Considering that existing studies fail to capture the correlation between the degradation rate and volatility of such load-sharing systems, this paper presents a novel load-sharing system with dependent degradation rate and volatility, reliability modelling and evaluation for which are worthy of investigation.

In the realm of reliability engineering, one of the primary objectives of system reliability assessment is to serve as a pivotal input for maintenance strategy optimization. Maintenance modelling for multi-unit systems typically necessitates the consideration of stochastic dependence [14] and economic dependence [15] among the consisting components. For load-sharing systems, inter-unit load correlation manifests as a specific form of stochastic dependencies, indicating that the failure of any unit in the system will impact the following degradation processes of surviving units [16], which complicates the system maintenance modelling and optimization. Considering the stochastic and economic dependence among units, Endharta and Ko studied the corrective and preventive maintenance strategy optimization models of circular balanced load-sharing systems [17]. Keizer et al. proposed an optimal replacement strategy for load-sharing systems subject to discrete Markovian degradation models [18]. Employing the Gamma process to describe the monotonic degradation process of units, Uit Het Broek et al. achieved joint optimization of production and maintenance strategies for load-sharing systems [19].

Furthermore, owing to considerable but sharable maintenance set-up cost, the economic dependence between different units in a load-sharing system should also be considered to improve the efficiency of intelligent maintenance [20]. As a most representative maintenance strategy to address economic dependence, opportunistic maintenance (OM) is designed to perform maintenance actions on units meeting specific control limit criteria during opportunity windows created by timely maintenance on other units [21]. Initially studied by Radner and Jorgenson [22], the investigation of OM for multi-unit systems has received widespread attention over the past years. Under a general unit lifetime distribution, Laggoune et al. introduced an OM policy for multi-unit series systems with data uncertainty, and minimized the expected replacement cost [23]. For a general multi-unit system consisting of identical units with economic dependence, Zhang and Zeng carried out OM under partitioning deterioration state spaces [24]. Vu et al. introduced a general OM strategy for multi-unit redundant systems, like parallel, k-out-of-n and parallel-series systems [25]. In pursuit of profit maximization, Xia et al. devised a novel OM strategy tailored for intricate series-parallel leased systems [26]. Utilizing Gamma processes for main unit degradation modelling and assuming exponential distribution for auxiliary unit lifetimes, Cai et al. conducted opportunistic inspections for systems with load-sharing auxiliary units [27].

In general, the regenerative process is usually adapted to describe the system degradation and maintenance process. For the traditional single-unit system, the regenerative process is often used to emphasize that the system degrades from its initial state, usually referred to as the perfect state: degradation level = 0, until it undergoes maintenance, after which its state is restored to the initial condition, marking the completion of one

complete renewal cycle and restarting a new one [28-30]. However, for multi-unit systems, a complete renewal cycle generally requires simultaneous maintenance of all units to restore the system to its initial state. Considering the possibility of only maintaining some of the units at the moments of inspection and decision-making, it is a tedious task of determining the renewal cycle due to the complex degradation process of multi-unit systems [31]. Under this circumstance, the semi-regenerative process is introduced by modelling the stationary distribution π, and allowing for a system semi-regenerative cycle in accordance with the inspection cycle, i.e., a new system semi-regenerative cycle begins from multiple steady states at each inspection moment [32]. This approach significantly makes the analysis of maintenance behavior for multi-unit systems more simplified and feasible [33]. Castanier et al. applied the semi-regenerative process to the maintenance modeling of two-unit series systems, gaining significant recognition [34]. Zhou et al. utilized the semi-regenerative process for maintenance optimization of multi-state series parallel system studies [35].

Therefore, motivated by a laser system example with specific system-level output power requirements and a positive correlation between laser degradation rate and volatility, this paper develops a novel load-sharing system with general degradation rate-volatility-load correlation, and derives the system reliability by addressing the effects of unit load on both degradation rate and volatility. Furthermore, to fill the gap of maintenance for load-sharing systems with economic dependency, the OM strategy is introduced for the developed novel load-sharing systems, and further optimized based on the semi-regenerative process to obtain the optimal inspection interval, the PM and OM threshold levels. The rest of the paper is planned as follows. In Section 2, the degradation modelling of the unit and the reliability evaluation of the load-sharing system is carried out. In Section 3, the OM strategy is modelled and optimized based on the semi-regenerative process. Numerical examples and sensitivity analyses are studied in Section 4 to demonstrate the effectiveness and robustness of our proposed strategy. Section 5 summarizes this paper.

2. Reliability model

2.1. Unit degradation modelling

In this Section, a two-unit load-sharing system will be analyzed, where the non-monotonic degradation process of each unit is described by the Wiener processes. The main assumptions of the model are as follows:

At time t, the degradation states of unit i $(i = 1, 2)$ can be characterized by:

$$X_i(t) = \mu_i t + \sigma_i B(t) \tag{1}$$

Where μ_i is the drift parameter, σ_i is the diffusion parameter, and $B(\cdot)$ represents the standard Brownian motion.

Due to the dependence of the unit degradation rate on the magnitude of the shared load (seen as an accelerating stress) [17], we assume that μ_i is a monotonically increasing function with respect to the load magnitude $L_i(L_i = \alpha_i L)$ shared by unit i, where α_i is the unit load-sharing factor, i.e., the sharing load proportion of unit i, and satisfying that $\alpha_1 + \alpha_2 = 1$. Without loss of generosity, the degradation rate-load correlation model is assumed to be:

$$\mu_i = \varphi_i(L_i) \tag{2}$$

Motivated by the mentioned laser system example with specific output power requirements, the unit degradation rate and volatility in the developed novel load-sharing system are assumed to be positively correlated. Without loss of generosity, the degradation rate-volatility correlation model and the resulting degradation volatility-load correlation model are assumed to be:

$$\sigma_i = \vartheta_i(\mu_i) = \vartheta_i\big(\varphi_i(L_i)\big) \tag{3}$$

It is assumed that unit i $(i = 1, 2)$ fails when its degradation value exceeds a failure threshold D_i. Furthermore, the system breaks down when the degradation values of both units exceed D_i.

Considering the characteristics of the Wiener process, the first-passage time T_i when unit i $(i = 1, 2)$ first reaches the threshold D_i follows an inverse Gaussian distribution. The corresponding probability density function (PDF) and cumulative distribution function (CDF) of this distribution for two-unit load-sharing systems can be expressed as:

$$f_{T_i}(t) = \frac{D_i}{\sqrt{2\pi[\vartheta_i(\varphi_i(L_i))]^2 t^3}} exp\left\{-\frac{(D_i-\varphi_i(L_i)t)^2}{2[\vartheta_i(\varphi_i(L_i))]^2 t}\right\} \tag{4}$$

$$F_{T_i}(t) = \Phi\left(\frac{\varphi_i(L_i)t - D_i}{[\vartheta_i(\varphi_i(L_i))]\sqrt{t}}\right) + exp\left(-\frac{2\varphi_i(L_i)D_i}{[\vartheta_i(\varphi_i(L_i))]^2}\right)\Phi\left(-\frac{\varphi_i(L_i)t + D_i}{[\vartheta_i(\varphi_i(L_i))]\sqrt{t}}\right) \quad (5)$$

2.2. System reliability evaluation

The redundant feature of load-sharing systems ensures that as long as one unit is functioning, the system can operate normally. Based on the above unit degradation models, the lifetime distribution CDF of the novel load-sharing system with dependent degradation rate and volatility can be further derived through the following two scenarios:

$$\begin{aligned} F_S(t) &= P_t\{\text{Both two units failed before time } t\} \\ &= P_t\{B\text{efore time } t, \text{unit 1 failed first and unit 2 failed later}\} \\ &+ P_t\{\text{Before time } t, \text{unit 2 failed first and unit 1 failed later}\} \\ &= F_{S1}(t) + F_{S2}(t) \end{aligned} \quad (6)$$

The descriptions of two different scenarios and the corresponding probability derivations are presented as follows:

Scenario 1: Under a proportionally allocated load magnitude, i.e., $\alpha_1 L$ and $(1-\alpha_1)L$ respectively, the consisting two units operate normally at the initial working time. Due to the heterogeneity of the unit degradation processes, unit 1 fails first at some random moment τ in $(0, t)$. Thereafter, the load of unit 1 is transferred to unit 2, causing an acceleration in both degradation rate and volatility of unit 2. Under full system load, unit 2 eventually fails before time t, leading to the failure of the entire load-sharing system. Therefore, considering the above degradation processes, $F_{S1}(t)$ in Equation (6) can be derived as:

$$F_{S1}(t) = \int_0^t \int_\tau^t f_{(1)T_2}(s)ds \cdot f_{(1)T_1}(\tau)d\tau = \int_0^t P(\tau < T_2 < t) f_{(1)T_1}(\tau)d\tau \quad (7)$$

Where $f_{(1)T_i}(\cdot)$ is the lifetime distribution of unit i $(i = 1, 2)$ in scenario 1.

For unit 1 working until failure under the predefined load $\alpha_1 L$, its lifetime distribution in Scenario 1 can be readily obtained through Equation (4). However, unit 2 undergoes two-phase degradation processes due to load reallocation, making it challenging to determine its lifetime distribution. Here, we assume $x_{2,\tau}$ as the degradation value of unit 2 at the change point τ. Given τ is a random variable in $(0, t)$, $x_{2,\tau}$ is also unknown under the constraint of not exceeding the failure threshold D_i. Let the transition probability function be $g(x_{2,\tau})$, denoting the probability density of degradation value of unit 2 from initial value 0 to $x_{2,\tau}$, which can be described as [36]:

$$g(x_{2,\tau}) = \frac{1}{\sqrt{2\pi\tau\sigma_{2,1}^2}}\left\{exp\left[-\frac{(x_{2,\tau}-\mu_{2,1}\tau)^2}{2\sigma_{2,1}^2\tau}\right] - exp\left[\frac{2D_2\mu_{2,1}}{\sigma_{2,1}^2}\right]\cdot exp\left[-\frac{(x_{2,\tau}-2D_2-\mu_{2,1}\tau)^2}{2\sigma_{2,1}^2\tau}\right]\right\} \quad (8)$$

Where $\mu_{2,1} = \varphi_2(L_2)$ and $\sigma_{2,1} = \vartheta_2(\varphi_2(L_2))$, representing the drift parameter and diffusion parameter of unit 2 in the first degradation process with shared load $L_2 = (1-\alpha_1)L$. Based on the analytical formula of $g(x_{2,\tau})$ in Equation (8), we can further derive the lifetime distribution of unit 2 in scenario 1 as follows:

$$\begin{aligned} f_{(1)T_2}(s) &= \int_{-\infty}^{D_2} f_{(1)T_2}(s|x_{2,\tau})\, g(x_{2,\tau})dx_{2,\tau} = \int_{-\infty}^{D_2} \frac{D_2 - x_{2,\tau}}{\sqrt{2\pi\sigma_{2,2}^2(s-\tau)^3}} exp\left[-\frac{(D_2 - x_{2,\tau} - \mu_{2,2}(s-\tau))^2}{2\sigma_{2,2}^2(s-\tau)}\right] \times \\ &\frac{1}{\sqrt{2\pi\tau[\vartheta_2(\varphi_2(L_2))]^2}}\left\{exp\left[-\frac{(x_{2,\tau}-\varphi_2(L_2)\tau)^2}{2[\vartheta_2(\varphi_2(L_2))]^2\tau}\right] - exp\left[\frac{2D_2\varphi_2(L_2)}{[\vartheta_2(\varphi_2(L_2))]^2}\right] exp\left[-\frac{(x_{2,\tau}-2D_2-\varphi_2(L_2)\tau)^2}{2[\vartheta_2(\varphi_2(L_2))]^2\tau}\right]\right\} dx_{2,\tau} = \\ &\frac{D_2}{\sqrt{[\vartheta_2(\varphi_2(L_2))]^2\pi(s-\tau)^2\tau + \sigma_{2,2}^2\pi(s-\tau)^3}}\left\{ e^A \Phi\left[\frac{D_2 - \frac{\tau\left(D_2[\vartheta_2(\varphi_2(L_2))]^2 + (s-\tau)(\sigma_{2,2}^2\varphi_2(L_2) - [\vartheta_2(\varphi_2(L_2))]^2\mu_{2,2})\right)}{\tau[\vartheta_2(\varphi_2(L_2))]^2 + (s-\tau)\sigma_{2,2}^2}}{\sqrt{\frac{2[\vartheta_2(\varphi_2(L_2))]^2\sigma_{2,2}^2(s-\tau)\tau}{\tau[\vartheta_2(\varphi_2(L_2))]^2 + (s-\tau)\sigma_{2,2}^2}}}\right] - exp\left[\frac{2D_2\varphi_2(L_2)}{\sigma_2^2} + \right.\right. \\ &\left.\left. B\right]\Phi\left[\frac{D_2 - \frac{\left(\tau[\vartheta_2(\varphi_2(L_2))]^2(D_2 - \mu_{2,2}(s-\tau)) + (s-\tau)\sigma_{2,2}^2(2D_2 + \varphi_2(L_2)\tau)\right)}{\tau[\vartheta_2(\varphi_2(L_2))]^2 + (s-\tau)\sigma_{2,2}^2}}{\sqrt{\frac{2[\vartheta_2(\varphi_2(L_2))]^2\sigma_{2,2}^2(s-\tau)\tau}{\tau[\vartheta_2(\varphi_2(L_2))]^2 + (s-\tau)\sigma_{2,2}^2}}}\right]\right\} + \frac{1}{2\pi\vartheta_2(\varphi_2(L_2))\sigma_{2,2}\sqrt{(s-\tau)^3\tau}}\left\{exp\left[A - \right.\right. \\ &\left.\left.\frac{\left[D_2 - \frac{\tau\left(D_2[\vartheta_2(\varphi_2(L_2))]^2 + (s-\tau)(\sigma_{2,2}^2\varphi_2(L_2) - [\vartheta_2(\varphi_2(L_2))]^2\mu_{2,2})\right)}{\tau[\vartheta_2(\varphi_2(L_2))]^2 + (s-\tau)\sigma_{2,2}^2}\right]^2}{\frac{2[\vartheta_2(\varphi_2(L_2))]^2\sigma_{2,2}^2(s-\tau)\tau}{\tau[\vartheta_2(\varphi_2(L_2))]^2 + (s-\tau)\sigma_{2,2}^2}}\right] - exp\left[\frac{2D_2\varphi_2(L_2)}{\sigma_2^2} + B - \frac{\left[D_2 - \frac{\left(\tau[\vartheta_2(\varphi_2(L_2))]^2(D_2 - \mu_{2,2}(s-\tau)) + (s-\tau)\sigma_{2,2}^2(2D_2 + \varphi_2(L_2)\tau)\right)}{\tau[\vartheta_2(\varphi_2(L_2))]^2 + (s-\tau)\sigma_{2,2}^2}\right]^2}{\frac{2[\vartheta_2(\varphi_2(L_2))]^2\sigma_{2,2}^2(s-\tau)\tau}{\tau[\vartheta_2(\varphi_2(L_2))]^2 + (s-\tau)\sigma_{2,2}^2}}\right]\right\} \end{aligned} \quad (9)$$

Where:

$$A = \frac{[\vartheta_2(\varphi_2(L_2))]^2 D_2\tau + (s\tau - \tau^2)(\sigma_{2,2}^2\varphi_2(L_2) - [\vartheta_2(\varphi_2(L_2))]^2\mu_{2,2})}{2[\vartheta_2(\varphi_2(L_2))]^4\sigma_{2,2}^2(s-\tau)\tau^2 + 2[\vartheta_2(\varphi_2(L_2))]^2\sigma_{2,2}^4(s-\tau)^2\tau}$$
$$- \frac{\left(\tau[\vartheta_2(\varphi_2(L_2))]^2 + (s-\tau)\sigma_{2,2}^2\right)\left([\vartheta_2(\varphi_2(L_2))]^2\tau\left(D_2 - \mu_{2,2}(s-\tau)\right)^2 + (s-\tau)\sigma_{2,2}^2[\vartheta_2(\varphi_2(L_2))]^2\tau^2\right)}{2[\vartheta_2(\varphi_2(L_2))]^4\sigma_{2,2}^2(s-\tau)\tau^2 + 2[\vartheta_2(\varphi_2(L_2))]^2\sigma_{2,2}^4(s-\tau)^2\tau}$$

$$B = -\frac{\left(\tau[\vartheta_2(\varphi_2(L_2))]^2 + (s-\tau)\sigma_{2,2}^2\right)\left[\tau[\vartheta_2(\varphi_2(L_2))]^2\left(D_2 - \mu_{2,2}(s-\tau)\right)^2 + (s-\tau)\sigma_{2,2}^2(2D_2 + \varphi_2(L_2)\tau)^2\right]}{2[\vartheta_2(\varphi_2(L_2))]^4\sigma_{2,2}^2(s-\tau)\tau^2 + 2[\vartheta_2(\varphi_2(L_2))]^2\sigma_{2,2}^4(s-\tau)^2\tau}$$
$$+ \frac{\left(\tau[\vartheta_2(\varphi_2(L_2))]^2\left(D_2 - \mu_{2,2}(s-\tau)\right) + (s-\tau)\sigma_{2,2}^2(2D_2 + \varphi_2(L_2)\tau)\right)^2}{2[\vartheta_2(\varphi_2(L_2))]^4\sigma_{2,2}^2(s-\tau)\tau^2 + 2[\vartheta_2(\varphi_2(L_2))]^2\sigma_{2,2}^4(s-\tau)^2\tau}$$

and $\mu_{2,2} = \varphi_2(L), \sigma_{2,2} = \vartheta_2(\varphi_2(L))$ represent the drift parameter and diffusion parameter of unit 2 in the second-phase degradation process under total system load L, and the derivation for Equation (9) is provided in Appendix A.1.

Scenario 2: In contrast to Scenario 1, unit 2 fails first in Scenario 2, followed by unit 1 before time t, leading to system failure. Therefore, unit 2 experiences the degradation process under load $(1-\alpha_1)L$ until random failure time ω, which is also the change point for unit 1 experiencing a two-phase degradation process, one under load $\alpha_1 L$ and the other under full load L. Taking accounting for the random failure time ω for unit 2, and random failure time $\zeta \in (\omega, t)$ for unit 1, the system lifetime CDF in Scenario 2 can be defined in Equation (10) and obtained by straightly following the derivation of Equation (9), thus omitted here.

$$\begin{aligned} F_{S2}(t) &= \int_0^t \int_\omega^t f_{(2)T_1}(\zeta)d\zeta \cdot f_{(2)T_2}(\omega)d\omega \\ &= \int_0^t P(\omega < T_1 < t) f_{(2)T_2}(\omega)d\omega \end{aligned} \quad (10)$$

Where $f_{(2)T_i}(\cdot)$ is the lifetime distribution of unit i $(i = 1, 2)$ in scenario 2.

By substituting Equations (7-10) into Equation (6), the system reliability and failure time distribution can be obtained to calculate the downtime cost in case of system failure in subsequent maintenance modelling and optimization.

3. Opportunistic maintenance strategy

Traditional CBM strategy usually performs PM or CM separately on each unit, when its own inspection degradation state exceeds a given threshold level. However, for load-sharing systems with economic dependence among units, considerable and shareable set-up cost indicate that collectively maintaining multiple units simultaneously may incur lower maintenance cost. Opportunistic maintenance (OM), referring to maintaining a working unit that satisfies specific control limit criteria (such as degradation levels not exceeding the PM threshold but already falling within opportunistic threshold ranges), offers the opportunity to conduct maintenance activities on multiple units during the window period generated by PM or CM on one unit, thus leading to set-up cost reduction and future system failure decline. Therefore, this Section introduces the OM strategy for load-sharing systems with economic dependence, which is optimized by minimizing the long-run average cost rate based on the semi-regenerative process.

3.1. Maintenance strategies and associated cost

Denote $\{t_k, k = 1,2, \dots, N\}$ as the periodical inspection time points, and $X_i(t_k)$ represents the degradation state of unit i $(i = 1, 2)$ at the corresponding moment, where the constant inspection interval δ is a decision variable to be optimized. Based on the degradation states of the units $(x_{i,k}, i = 1,2)$ obtained at the detection time t_k, the maintenance interventions are primarily classified into corrective maintenance (CM), preventive maintenance (PM) and opportunistic maintenance (OM) with the corresponding control limit threshold levels, i.e., D_i, M_{Pi} and M_{Oi} (usually under the assumption that $M_{Oi} < M_{Pi} < D_i$), respectively. For an individual unit i, when the degradation level falls within the range $[0, M_{Pi})$, no maintenance action is taken. When the degradation level falls within the range $[M_{Pi}, D_i)$, PM is conducted. And when the degradation level exceeds D_i, CM is performed. Furthermore, if PM or CM is scheduled for one unit at some inspection time point, OM will be conducted on other units whose degradation levels exceed M_{Oi} but are smaller than M_{Pi}. All the maintenance interventions and corresponding control limit threshold levels are shown in Figure 1.

Performing CM incurs the highest cost, denoted as c_C, while

both PM and OM fall under the category of proactive maintenance to prevent system failures, with the same cost denoted as c_P. Additionally, c_I denotes the cost for each inspection to detect the system state of the system. Furthermore, maintenance on a load-sharing system generally requires relevant preparation and set-up work, the cost of which is denoted as c_S. Interestingly, when multiple units undergo maintenance simultaneously, these set-up tasks can be shared, resulting in a one-time set-up cost [37]. Considering that system failures can only be observed through periodic inspections, system operation in failure state will lead to economic losses recorded as downtime cost c_d.

The maintenance strategies and corresponding maintenance cost for a two-unit load-sharing system can be intuitively shown in Figure 1, and comprehensively described through the following eight scenarios, where $k = 1,2,\dots,N$ stands for the inspection order and $i = 1,2;\ j = 1,2;\ i \neq j$ are the numbers of unit.

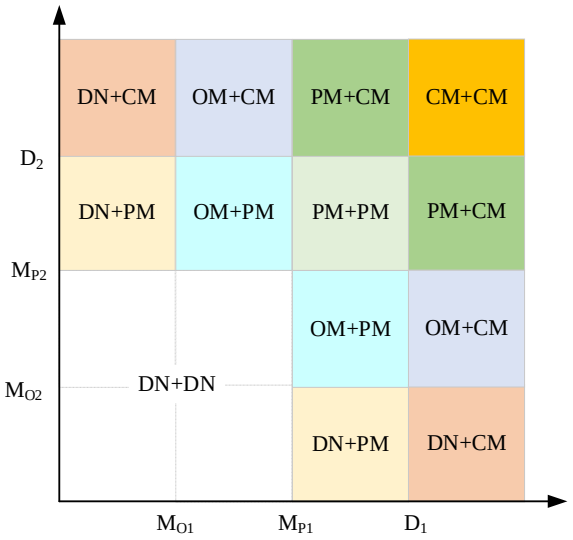

Figure 1. Maintenance interventions and corresponding control limit threshold levels.

Scenario 1: $x_{i,k} \leq M_{Pi}\ and\ x_{j,k} \leq M_{Pj}$: No maintenance is performed on either unit, incurring only inspection cost c_I, and the next degradation cycle starts with unchanged system state.

Scenario 2: $x_{i,k} \leq M_{Oi}\ and\ M_{Pj} < x_{j,k} \leq D_j$: Unit i undergoes no maintenance, while PM is conducted on unit j, incurring total cost $(c_S + c_I + c_P)$. Post-maintenance, unit i remains unchanged while unit j is restored to a state as good as new.

Scenario 3: $x_{i,k} \leq M_{Oi}\ and\ x_{j,k} > D_j$: Unit i undergoes no maintenance, while CM is performed on unit j, incurring total cost $(c_S + c_I + c_C)$. Post-maintenance, unit i remains unchanged while unit j is restored to a state as good as new.

Scenario 4: $M_{Oi} < x_{i,k} \leq M_{Pi}\ and\ M_{Pj} \leq x_{j,k} \leq D_j$: OM is carried out on unit i, and PM is conducted on unit j, incurring total cost $(c_S + c_I + 2c_P)$. Post-maintenance, both units are restored to states as good as new.

Scenario 5: $M_{P1} < x_{1,k} \leq D_1\ and\ M_{P2} < x_{2,k} \leq D_2$: PM is carried out on both unit 1 and unit 2, incurring total cost $(c_S + c_I + 2c_P)$. Post-maintenance, both units are restored to states as good as new.

Scenario 6: $M_{Oi} \leq x_{i,k} \leq M_{Pi}\ and\ x_{j,k} \geq D_j$: OM is conducted on unit i, while CM is performed on unit j, incurring cost $(c_S + c_I + c_P + c_C)$. Post-maintenance, both units are restored to states as good as new.

Scenario 7: $M_{Pi} \leq x_{i,k} \leq D_i\ and\ x_{j,k} \geq D_j$: PM is conducted on unit i, while CM is performed on unit j, incurring cost $(c_S + c_I + c_P + c_C)$. Post-maintenance, both units are restored to states as good as new.

Scenario 8: $x_{1,k} \geq D_1\ and\ x_{2,k} \geq D_2$: CM is performed on both unit 1 and unit 2, incurring total cost $(c_S + c_I + 2c_C + c_d \cdot t_{down})$. Post-maintenance, both units are restored to states as good as new.

where t_{down} denotes the system downtime length.

3.2. Stationary distribution of the maintained system states

Considering that the conventional renewal process appears tedious when modelling and optimizing maintenance strategies for multi-unit systems [32], the inspection-maintenance process of load-sharing systems can be effectively modelled and described by the popular semi-regenerative process [34]. Unlike the singular initial state in the renewal process, the semi-regenerative process allows for multiple initial states to commence a new degradation cycle. An embedded Markov chain $\{X_i(t_k), k = 1,2,\dots,N\}$ is incorporated to depict the degradation levels of unit i $(i = 1,2)$ at various inspection instants (prior to maintenance) t_k for the semi-regenerative process $\{X_i(t), t > 0\}$, where the semi-regenerative cycle is determined and aligns with each inspection interval δ. Denote the stationary distribution of the embedded Markov chain as π, the existence of which is proven utilizing the properties of

Harris recurrent, and is stated in the following Lemma 1.

Lemma 1. *The Markov chain* $\{X_i(t_k), k = 1, 2, \dots, N; i = 1,2\}$ *is Harris recurrent*.

The proof of Lemma 1 is provided in Appendix A.2. Based on Lemma 1, we can ascertain the existence of the stationary distribution π for the state evolution process of the load-sharing system under maintenance at inspection times (prior to maintenance). Furthermore, the stationary distribution π can be derived through systematic analysis of all potential maintenance scenarios (as described in subsection 3.1) within a semi-regenerative cycle δ.

Considering two consecutive inspection times (prior to maintenance), i.e., semi-regenerative instants, where the current degradation states of the load-sharing system with two units are denoted as (x_1, x_2) and their degradation states at the next regenerative point as (y_1, y_2). Based on all maintenance scenarios described in subsection 3.1, the stationary distribution π of the system degradation states can be derived as follows:

$$\pi(y_1, y_2) = \underbrace{\int_{-\infty}^{M_{P2}} \int_{-\infty}^{M_{P1}} \pi(x_1, x_2)\, f_{Z_1,Z_2}(y_1 - x_1, y_2 - x_2) dx_1 dx_2}_{Scenario\ 1} + \underbrace{\int_{0}^{M_{O1}} \int_{M_{P2}}^{+\infty} \pi(x_1, x_2)\, f_{Z_1,Z_2}(y_1 - x_1, y_2) dx_2 dx_1}_{Scenario\ 2a+Scenario\ 3a} +$$
$$\underbrace{\int_{0}^{M_{O2}} \int_{M_{P1}}^{+\infty} \pi(x_1, x_2)\, f_{Z_1,Z_2}(y_1, y_2 - x_2) dx_1 dx_2}_{Scenario\ 2b+Scenario\ 3b} + \underbrace{\int_{M_{O2}}^{M_{P2}} \int_{M_{P1}}^{+\infty} \pi(x_1, x_2)\, f_{Z_1,Z_2}(y_1, y_2) dx_1 dx_2}_{Scenario\ 4a+Scenario\ 6a} +$$
$$\underbrace{\int_{M_{O1}}^{M_{P1}} \int_{M_{P2}}^{+\infty} \pi(x_1, x_2)\, f_{Z_1,Z_2}(y_1, y_2) dx_2 dx_1}_{Scenario\ 4b+Scenario\ 6b} + \underbrace{\int_{M_{P2}}^{\infty} \int_{M_{P1}}^{\infty} \pi(x_1, x_2)\, f_{Z_1,Z_2}(y_1, y_2) dx_1 dx_2}_{Scenario\ 5+Scenario\ 7+Scenario\ 8} \quad (11)$$

The interpretation of Equation (11) is as follows: in Scenario 1, the system degradation state at the current inspection point is (x_1, x_2), and no maintenance is performed. The observed system degradation state at the next inspection point (prior to maintenance) is (y_1, y_2). In other words, the degradation increment of the system within this semi-regenerative cycle δ is denoted as $(y_1 - x_1, y_2 - x_2)$ in Equation (11). Similarly, Scenario 2 can be analyzed by assuming that the current system degradation state is (x_1, x_2) and satisfies condition $x_1 \leq M_{O1}\ and\ M_{P2} < x_2 \leq D_2$. In this case, no maintenance is performed on unit 1, while preventive maintenance is conducted on unit 2. After maintenance, the system state is renewed as $(x_1, 0)$. After one inspection cycle δ, the system state at the inspection point (prior to maintenance) is (y_1, y_2), and the degradation increment within this semi-regenerative cycle δ is denoted as $(y_1 - x_1, y_2)$. Likewise, the interpretation of the other scenarios in Equation (11) can be similarly elucidated.

Furthermore, $f_{Z_1,Z_2}(\cdot,\cdot)$ in Equation (11) is the joint PDF of system degradation increments during a regenerative cycle δ and let the increments be (z_1, z_2) for simplicity. Due to the properties of load-sharing systems, the stochastic dependencies among components will pose challenges in deriving the joint distribution function of degradation increments. Assuming that units fail upon reaching the failure threshold D_i for the first time and their degradation states remain unchanged thereafter, the corresponding joint cumulative distribution function (CDF) $F_{Z_1,Z_2}(z_1, z_2)$ can be derived under the following three scenarios:

$$F_{Z_1,Z_2}(z_1, z_2) = P\{Z_1 \leq z_1, Z_2 \leq z_2\} = F^1_{Z_1,Z_2}(z_1, z_2) + F^2_{Z_1,Z_2}(z_1, z_2) + F^3_{Z_1,Z_2}(z_1, z_2) = P\{Z_1 \leq z_1, Z_2 \leq z_2 | T_1 \geq \delta, T_2 \geq \delta\} P\{T_1 \geq \delta, T_2 \geq \delta\} +$$
$$P\{Z_1 \leq z_1, Z_2 \leq z_2 | T_1 < \delta, T_2 \geq \delta\} P\{T_1 < \delta, T_2 \geq \delta\} + P\{Z_1 \leq z_1, Z_2 \leq z_2 | T_1 \geq \delta, T_2 < \delta\} P\{T_1 \geq \delta, T_2 < \delta\} \quad (12)$$

Scenario 1: $T_1 \geq \delta, T_2 \geq \delta$

In this scenario, both units operate independently throughout the entire semi-regenerative cycle δ. Due to the characteristics of the Wiener degradation processes, the degradation increment of each unit within the inspection cycle δ obeys a normal distribution, and the first-passage-lifetime of each unit follows an inverse Gaussian distribution. Therefore, The joint CDF $F^1_{Z_1,Z_2}(z_1, z_2)$ in this scenario can be further derived as follows:

$$F^1_{Z_1,Z_2}(z_1, z_2) = P\{Z_1 \leq z_1, Z_2 \leq z_2 | T_1 \geq \delta, T_2 \geq \delta\} \cdot P\{T_1 \geq \delta, T_2 \geq \delta\} = \int_{-\infty}^{z_1} \int_{-\infty}^{z_2} f_1(u_1|\delta) f_2(u_2|\delta) du_1 du_2 \cdot$$
$$\int_{\delta}^{\infty} \int_{\delta}^{\infty} g_1(s_1) g_2(s_2) ds_1 ds_2 = \Phi\left[\frac{z_1 - \varphi_1(L_1)\delta}{\vartheta_1(\varphi_1(L_1))\sqrt{\delta}}\right]\left[\Phi\left(\frac{D_1 - \varphi_1(L_1)\delta}{\vartheta_1(\varphi_1(L_1))\sqrt{\delta}}\right) - exp\left(\frac{2\varphi_1(L_1)D_1}{[\vartheta_1(\varphi_1(L_1))]^2}\right) \cdot \Phi\left(-\frac{\varphi_1(L_1)\delta + D_1}{\vartheta_1(\varphi_1(L_1))\sqrt{\delta}}\right)\right] \times$$
$$\Phi\left[\frac{z_2 - \varphi_2(L_2)\delta}{\vartheta_2(\varphi_2(L_2))\sqrt{\delta}}\right]\left[\Phi\left(\frac{D_2 - \varphi_2(L_2)\delta}{\vartheta_2(\varphi_2(L_2))\sqrt{\delta}}\right) - exp\left(\frac{2\varphi_2(L_2)D_2}{[\vartheta_2(\varphi_2(L_2))]^2}\right) \cdot \Phi\left(-\frac{\varphi_2(L_2)\delta + D_2}{\vartheta_2(\varphi_2(L_2))\sqrt{\delta}}\right)\right] \quad (13)$$

Scenario 2: $T_1 < \delta, T_2 \geq \delta$

In this scenario, unit 1 fails midway during a semi-regenerative period δ, while unit 2 operates normally throughout the entire cycle. Considering the stochastic dependence between units and positive dependence between degradation rate and volatility in proposed load-sharing systems, after the failure of unit 1 at a random time point, not only the degradation rate of unit 2 is accelerated, but also its degradation volatility is intensified under full system load. Therefore, the joint CDF $F^2_{Z_1,Z_2}(z_1,z_2)$ can be further derived as follows:

$$F^2_{Z_1,Z_2}(z_1,z_2) = P\{Z_1 \leq z_1, Z_2 \leq z_2 | T_1 < \delta, T_2 \geq \delta\} \cdot P\{T_1 < \delta, T_2 \geq \delta\}$$

$$= \int_0^{\delta}\int_{-\infty}^{D_2}\int_{\delta}^{+\infty} P(Z_1(s_1) < z_1) \cdot P\left(z_{2,s_1} + Z_2(\delta - s_1) < z_2\right) \cdot f_{T_1}(s_1) \cdot g(z_{2,s_1}) \cdot f_{T_2}(s_2) ds_2 dz_{2,s_1} ds_1$$

$$= \int_0^{\delta}\int_{-\infty}^{D_2}\int_{\delta}^{+\infty} \Phi\left[\frac{z_2 - z_{2,s_1} - \varphi_2(L)(\delta - s_1)}{\vartheta_2(\varphi_2(L))\sqrt{\delta - s_1}}\right] \frac{D_2 - z_{2,s_1}}{\sqrt{2\pi[\vartheta_2(\varphi_2(L))]^2(s_2 - s_1)^3}} exp\left[-\frac{\left[D_2 - z_{2,s_1} - \varphi_2(L)(s_2 - s_1)\right]^2}{2[\vartheta_2(\varphi_2(L))]^2(s_2 - s_1)}\right] ds_2 \quad (14)$$

$$\times \frac{1}{\sqrt{2\pi\tau[\vartheta_2(\varphi_2(L_2))]^2}} \left\{exp\left[-\frac{\left(z_{2,s_1} - \varphi_2(L_2)s_1\right)^2}{2[\vartheta_2(\varphi_2(L_2))]^2 s_1}\right] - exp\left[\frac{2D_2\varphi_2(L_2)}{[\vartheta_2(\varphi_2(L_2))]^2}\right] \cdot exp\left[-\frac{\left(z_{2,s_1} - 2D_2 - \varphi_2(L_2)s_1\right)^2}{2[\vartheta_2(\varphi_2(L_2))]^2 s_1}\right]\right\} dz_{2,s_1} \times 1$$

$$\times \frac{D_1}{\sqrt{2\pi[\vartheta_1(\varphi_1(L_1))]^2 s_1^3}} exp\left[-\frac{[D_1 - \varphi_1(L_1)s_1]^2}{2[\vartheta_1(\varphi_1(L_1))]^2 s_1}\right] ds_1$$

Scenario 3: $T_1 \geq \delta, T_2 < \delta$

In this scenario, unit 2 fails midway during the semi-regenerative period δ, while unit 1 keeps operating normally. Similar to the above Scenario 2, the joint CDF can be further derived as follows:

$$F^3_{Z_1,Z_2}(z_1,z_2) = P\{Z_1 \leq z_1, Z_2 \leq z_2 | T_1 \geq \delta, T_2 < \delta\} \cdot P\{T_1 \geq \delta, T_2 < \delta\} = \int_0^{\delta}\int_{-\infty}^{D_1}\int_{\delta}^{+\infty} P(Z_2(s_2) < z_2) \cdot P\left(z_{1,s_2} + Z_1(\delta - s_2) < z_1\right) \cdot f_{T_2}(s_2) \cdot g\left(z_{1,s_2}\right) \cdot f_{T_1}(s_1) ds_1 \, dz_{1,s_2} ds_2 =$$

$$\int_0^{\delta}\int_{-\infty}^{D_1}\int_{\delta}^{+\infty} \Phi\left[\frac{z_1 - z_{1,s_2} - \varphi_1(L)(\delta - s_2)}{\vartheta_1(\varphi_1(L))\sqrt{\delta - s_2}}\right] \frac{D_1 - z_{1,s_2}}{\sqrt{2\pi\left[\vartheta_1(\varphi_1(L))\right]^2(s_1 - s_2)^3}} exp\left[-\frac{\left[D_1 - z_{1,s_2} - \varphi_1(L)(s_1 - s_2)\right]^2}{2\left[\vartheta_1(\varphi_1(L))\right]^2(s_1 - s_2)}\right] ds_1 \times$$

$$\frac{1}{\sqrt{2\pi\tau\left[\vartheta_1(\varphi_1(L_1))\right]^2}} \left\{exp\left[-\frac{\left(z_{1,s_2} - \varphi_1(L_1)s_2\right)^2}{2\left[\vartheta_1(\varphi_1(L_1))\right]^2 s_2}\right] - exp\left[\frac{2D_1\varphi_1(L_1)}{\left[\vartheta_1(\varphi_1(L_1))\right]^2}\right] \cdot exp\left[-\frac{\left(z_{1,s_2} - 2D_1 - \varphi_1(L_1)s_2\right)^2}{2\left[\vartheta_1(\varphi_1(L_1))\right]^2 s_2}\right]\right\} dz_{1,s_2} \times 1 \times$$

$$\frac{D_2}{\sqrt{2\pi[\vartheta_2(\varphi_2(L_2))]^2 s_2^3}} exp\left[-\frac{[D_2 - \varphi_2(L_2)s_2]^2}{2[\vartheta_2(\varphi_2(L_2))]^2 s_2}\right] ds_2 \quad (15)$$

Equation (11) primarily consists of a bi-dimensional integral, which is not straightforward to solve directly. Instead, we employ a commonly used successive approximation approach to obtain the stationary distribution π under constraint $\int_{-\infty}^{+\infty}\int_{-\infty}^{+\infty} \pi(y_1,y_2)dy_1dy_2 = 1$. This iterative numerical algorithm is provided as follows to continuously approach the solution through iteration:

Algorithm 1. The successive approximation method for calculating π.

Input: inspection interval τ, OM threshold M_O, PM threshold M_P and precision ϑ.

1. Initialization: Set an arbitrary initial stationary distribution meeting: $\int_{-\infty}^{+\infty}\int_{-\infty}^{+\infty} \pi(x_1,x_2)dy_1dy_2 = 1$ and $\pi(x_1,x_2) \geq 0$ for both x_1 and x_2;
2. Compute: Derive $f_{Z_1,Z_2}(z_1,z_2)$ based on Equation (12) for both z_1 and z_2;
3. Update: In the lth iteration, calculate $\pi^l(y_1,y_2)$ based on Equation (11) by changing $\pi(x_1,x_2)$ on the right side of Equation (11) with $\pi^{l-1}(y_1,y_2)$ and the one on the left side with $\pi^l(y_1,y_2)$;
4. Check: If $\max|\pi^l(y_1,y_2) - \pi^{l-1}(y_1,y_2)| < \vartheta$, the true value of $\pi(y_1,y_2)$ is finally gained. Otherwise, return to step 3.

Output: The stationary distribution π of $\{X_i(t_k), k = 1,2,\dots,N; i = 1,2\}$.

3.3. Long-run average cost rate

Based on the properties of the semi-regenerative process, the long-term average cost rate can be characterized by the asymptotic expected cost rate within a semi-renewal cycle δ, which is closely linked to the stationary distribution π. This relationship can be further formulated as follows:

$$C_\infty = \lim_{t\to\infty}\frac{C(t)}{t} = \frac{E_\pi(C_I(\delta))}{E_\pi(\delta)} + \sum_{i=1}^{2}\frac{E_\pi\left(C_P^i(\delta)\right)}{E_\pi(\delta)} + \sum_{i=1}^{2}\frac{E_\pi\left(C_C^i(\delta)\right)}{E_\pi(\delta)} - (c_I + c_S)\frac{E_\pi(N_B(\delta))}{E_\pi(\delta)} + \frac{E_\pi(C_F(\delta))}{E_\pi(\delta)} \quad (16)$$

Where:

- δ represents the constant semi-regenerative cycle (inspection interval).
- $E_\pi(C_I(\delta))$ represents the expected system inspection cost, expressed as follows:

$$E_\pi(C_I(\delta)) = \int_{-\infty}^{M_{P1}}\int_{-\infty}^{M_{P2}} c_I\pi(y_1, y_2)\, dy_2 dy_1 \quad (17)$$

- $E_\pi(C_P^i(\delta))$ represents the expected OM and PM costs for each unit, expressed as follows:

$$E_\pi\left(C_P^i(\delta)\right) = \int_{M_{P1}}^{D_1}\int_{M_{P2}}^{D_2}\left(c_I + c_S + c_P^i\right)\pi(y_1, y_2)\, dy_2 dy_1 + \sum_{i=1}^{2}\sum_{j=1}^{2}\int_{M_{Oi}}^{M_{Pi}}\int_{M_{Pj}}^{+\infty}\left(c_I + c_S + c_P^i\right)\pi(y_i, y_j)\, dy_j dy_i + \sum_{i=1}^{2}\sum_{j=1}^{2}\int_{M_{Pi}}^{D_i}\int_{D_j}^{+\infty}\left(c_I + c_S + c_P^i\right)\pi(y_i, y_j)\, dy_j dy_i \ (i \neq j) \quad (18)$$

- $E_\pi(C_C^i(\delta))$ represents the expected CM cost for each unit, expressed as follows:

$$E_\pi\left(C_C^i(\delta)\right) = \int_{D_1}^{+\infty}\int_{D_2}^{+\infty}\left(c_I + c_S + c_C^i\right)\pi(y_1, y_2)\, dy_2 dy_1 + \sum_{i=1}^{2}\sum_{j=1}^{2}\int_{D_i}^{+\infty}\int_{M_{Oj}}^{D_j}\left(c_I + c_S + c_C^i\right)\pi(y_i, y_j)\, dy_j dy_i \ (i \neq j) \quad (19)$$

- $E_\pi(N_B(\delta))$ represents the probability of both two units are maintained simultaneously (complete system maintenance). Considering the economic dependence among units, the inspection and set-up costs under this portion of probability need to be subtracted when performing opportunistic maintenance.

$$E_\pi\left(N_B(\delta)\right) = \int_{M_{P1}}^{+\infty}\int_{M_{P2}}^{+\infty}\pi(y_1, y_2)\, dy_2 dy_1 + \sum_{i=1}^{2}\sum_{j=1}^{2}\int_{M_{Oi}}^{M_{Pi}}\int_{M_{Pj}}^{+\infty}\pi(y_i, y_j)\, dy_j dy_i \ (i \neq j) \quad (20)$$

- $E_\pi\left(C_F(\delta)\right)$ represents the expected system downtime cost, expressed as follows:

$$E_\pi(C_F(\delta)) = c_d E_\pi(t_{down}) = c_d\left[\delta - \int_0^\delta t_S dF_S(t_S)\right] \quad (21)$$

where i,j represent the numbering of the two units in the system, and $i = 1,2;\ j = 1,2;\ i \neq j$. t_{down} denotes the system downtime length, and t_S represents the system failure time, whose cumulative distribution function is denoted by $F_S(\cdot)$ calculated by substituting Equations (7-10) into Equation (6) in subsection 2.2.

In summary, the long-run average cost rate of the load-sharing system under the semi-regenerative process can be determined and calculated by substituting Equations (17)-(21) into Equation (16). By optimizing the OM threshold M_O, PM threshold M_P, and inspection interval δ, lowest long-run average cost rate can be further obtained for load-sharing systems.

4. Numerical examples and case study

The developed load-sharing system with dependent degradation rate and volatility can be commonly found in many industrial practices. For instance, a positive correlation between degradation rate and volatility is observed for the popular GaAs laser example [12]. Therefore, when two GaAs lasers operate together to maintain stable system-level output power, the laser system can be viewed as a novel type of load-sharing system with dependent degradation rate and volatility, where an increase in unit laser load will result in larger degradation rate and degradation volatility.

In this Section, the developed OM strategy for the novel load-sharing system with dependent degradation rate and volatility is applied to a numerical example and a case study of two-unit GaAs laser systems. Compared with the traditional CBM strategy separately for each unit, the effectiveness of our proposed OM strategy is validated, and sensitivity analyses are conducted to demonstrate the robustness of the optimal OM strategy.

4.1. Numerical examples

For the illustrative GaAs laser system example with two load-sharing units, the Wiener process is used to describe the degradation process of each laser unit, and the degradation rate-load correlation model is assumed to follow a power law relationship, which is commonly employed as an accelerated model to depict the effect of bearing load [17]. Besides,

referring to the conclusion in [13], the dependence between degradation rate (drift parameter) and volatility (diffusion parameter) is assumed to follow a linear relationship. Specific forms of the two relation models are listed as follows:

$$\mu_i = \varphi_i(L_i) = a_i(\alpha_i L)^{b_i} \quad (22)$$

$$\sigma_i = \vartheta_i(\mu_i) = \lambda_i a_i(\alpha_i L)^{b_i} \quad (23)$$

where $\alpha_i (i = 1, 2)$ is the unit load-sharing factor satisfying $\alpha_1 + \alpha_2 = 1$. In the following analysis, the commonly used equal load allocation policy is adapted for the novel load-sharing system, i.e., $\alpha_1 = \alpha_2 = 0.5$. λ_i, a_i, b_i are surrogate parameters.

Due to individual heterogeneity and environmental factors, the degradation parameters of the two units are assumed to be slightly different. Under this consideration, the main parameter values for the numerical examples are determined artificially in Table 1, including cost parameters, failure threshold D, system workload L, degradation parameters a_i, b_i, correlation parameter λ_i and load-sharing factor α_i.

Table 1. Main parameter setting for the numerical examples.

Parameter	c_S	c_P	c_C	c_I	c_d	D	L	a_1/a_2	b_1/b_2	λ_1/λ_2	α_1
Value	300	400	2000	10	2000	50	10	0.19/0.18	1.2/1.1	0.59/0.57	0.5

As a comparative maintenance strategy for load-sharing systems, the traditional CBM strategy only schedules PM and CM separately for each unit, and neglects the economic dependence between units. By applying this popular maintenance strategy to the two-unit GaAs laser system example, we plot Figure 2 to show the relationship between the system long-run average cost rate and the two decision variables, i.e., PM threshold M_P and inspection interval δ. The surface of Figure 2 exhibits a concave minimum, indicating the presence of a global optimum solution for the CBM strategy. The optimal long-run average cost rate, which is attained at inspection interval 5.81 and PM threshold 40.74, is finally calculated to be 38.01.

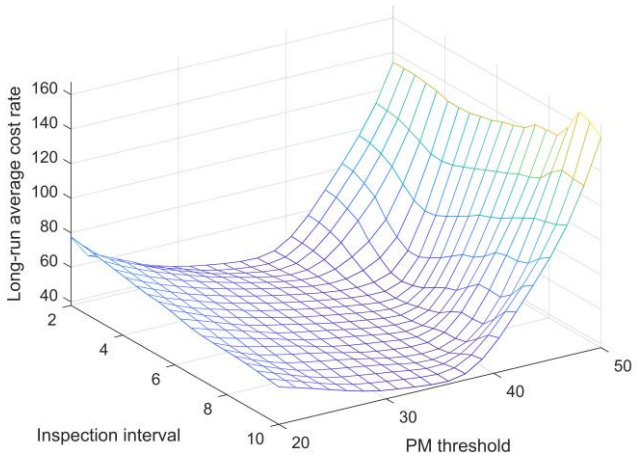

Figure 2. Long-run average cost rate with respect to M_P and δ under traditional CBM strategy.

In contrast to the traditional CBM strategy separately for each unit, the proposed OM strategy takes account of the economic dependence between units of the novel load-sharing system, which highlights the economic and practical significance of performing maintenance on the non-failed unit under the maintenance opportunity created by the failure of the other unit in the system. To apply the developed OM strategy for the numerical example, we first analyze the stationary distribution π for the system degradation states, which is approximately calculated by Algorithm 1 in subsection 3.2, and the average computation time is recorded to be 125s, with the convergence criterion of 0.001 (CPU: 11th Gen Intel(R) Core(TM) i7-11700 2.50GHz).

Let π_i $(i = 1, \ldots, 8)$ represent the probabilities of the system in Scenario i at an inspection point, as described in subsection 3.1. Based on a specific maintenance strategy $(\delta, M_O, M_P) = (4.22, 26.48, 42.21)$, the specific values of π under the proposed OM strategy can be calculated and shown as the Boxplot in Figure 3. Among the results, $E(\pi_1) = 0.8754$ indicates a higher probability of system healthy state, and also demonstrates that our proposed maintenance strategy can significantly improve system reliability. Since the inspection cost is relatively low, the higher frequency of Scenario 1 does not incur excessive economic cost. Furthermore, $E(\pi_4) = 0.1091$ indicates a high probability that the two units undergo maintenance simultaneously, in which case the set-up cost can be better saved, further validating the effectiveness of the proposed OM strategy. The rather smaller average values of π_3, π_6, π_7 and π_8 indicate that our proposed opportunistic

maintenance strategy effectively avoids system failures, significantly reducing the risks associated with downtime cost.

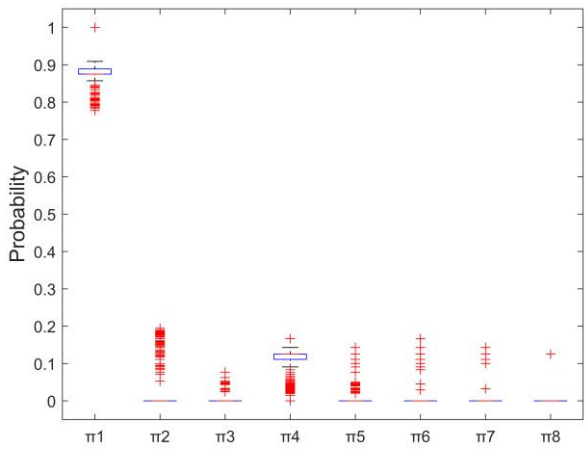

Figure 3. Boxplot of stationary distribution π under specific maintenance strategy $(\delta, M_O, M_P) = (4.22, 26.48, 42.21)$.

Based on the specific values of stationary distribution π, the developed OM strategy can be applied, where Figures 4-6 respectively show the system long-run average cost rate with respect to PM threshold M_P, OM threshold M_O, and inspection interval δ. Considering the presence of minima in all three figures, the minimum value of the long-run average cost rate is attained to be 34.94, with the corresponding optimal PM threshold as 42.21, OM threshold as 26.48, and inspection interval as 4.22. Compared to the traditional CBM strategy, a visible reduction (38.01 – 34.94)/38.01 = 8.08% in the long-run average cost rate can be obtained in our proposed OM strategy, indicating significant effectiveness of introducing opportunity maintenance for load-sharing systems to enhance system reliability and maintenance management practices.

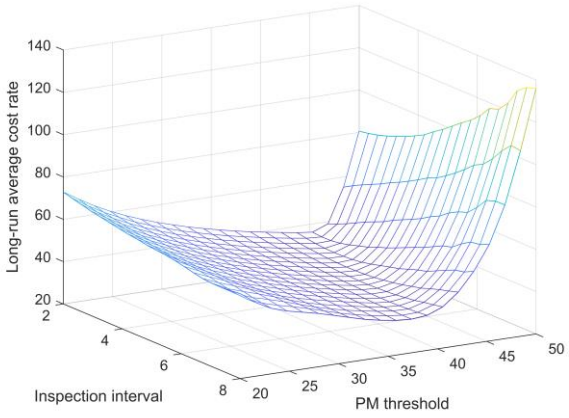

Figure 4. Long-run average cost rate with respect to M_P and δ under the proposed OM strategy.

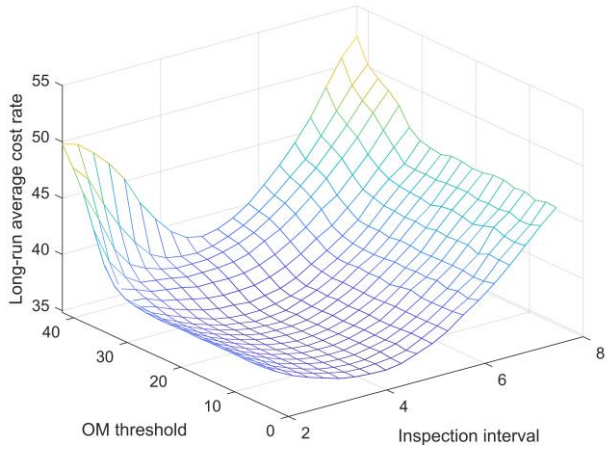

Figure 5. Long-run average cost rate with respect to M_O and δ under the proposed OM strategy.

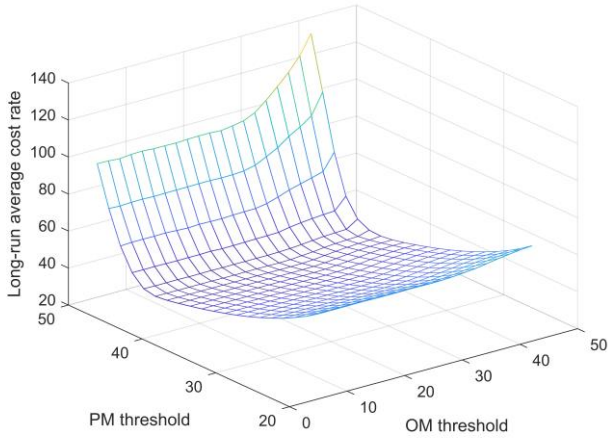

Figure 6. Long-run average cost rate with respect to M_O and M_P under the proposed OM strategy.

4.2. Sensitivity analysis

In this subsection, sensitivity analyses are conducted on representative degradation parameters and cost parameters for the optimal CBM and OM strategy, validating the robustness of the proposed new maintenance scheme for load-sharing systems. The main parameters analyzed include degradation parameters a, b, and correlation parameters λ, while the primary cost parameters analyzed include set-up cost c_S, PM cost c_P, CM cost c_C, and downtime cost c_d. The corresponding results are illustrated in Figures 7-13.

It can be visually observed that as degradation, correlation and cost parameters increase, the minimum long-run average cost rate also gradually increases, regardless of whether OM is incorporated or not. However, the difference lies in the fact that

with the introduction of OM, the cost rate consistently remains lower, indicating the effectiveness and robustness of our strategy.

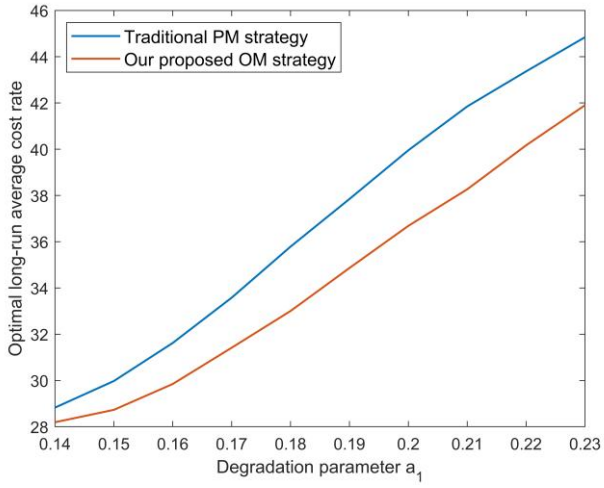

Figure 7. Sensitivity analysis on degradation parameter a_1.

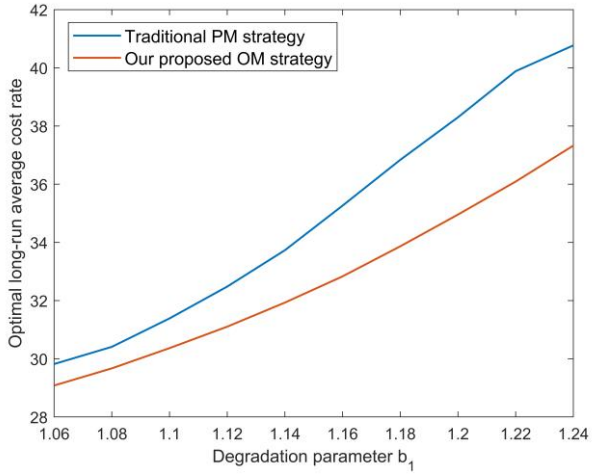

Figure 8. Sensitivity analysis on degradation parameter b_1.

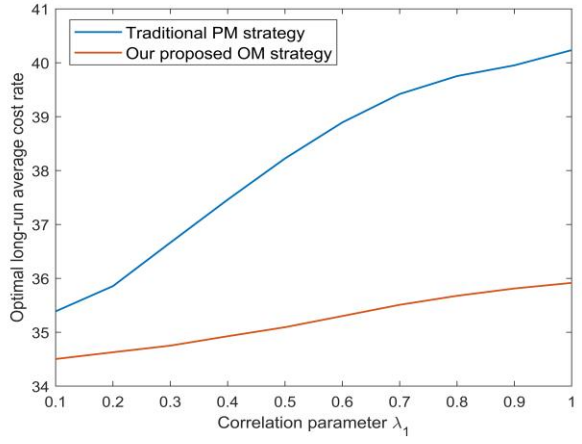

Figure 9. Sensitivity analysis on correlation parameter λ_1.

Furthermore, in case the set-up cost constitutes a large proportion of maintenance cost, the cost-effectiveness brought about by the OM strategy becomes more pronounced with the increase of c_S, as shown in Figure 10. Similar conclusions can be drawn regarding the impact of increasing CM cost in Figure 11. Additionally, it can be illustrated in Figure 12 that with the increase of PM cost, the economic benefit of conducting PM or OM in advance becomes smaller, and the two curves tend to converge when PM cost exceeds the potential cost caused by system failure, including the CM cost and downtime cost, and the optimal decision tends to be pure CM under both maintenance strategies. Figure 13 shows the impact of increased downtime cost on the long-run average cost rate, where the introduction of OM strategy reduces the system failure risk and narrows the average system downtime length. As a result, with the increase of downtime cost, the minimum long-run cost rate does not rise sharply but rather shows a gradual upward trend.

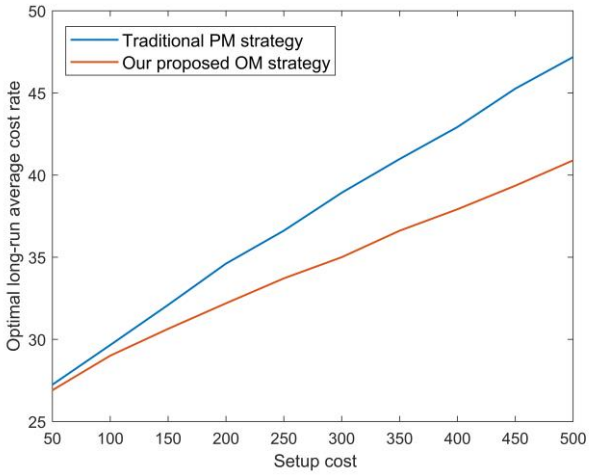

Figure 10. Sensitivity analysis on set-up cost c_S.

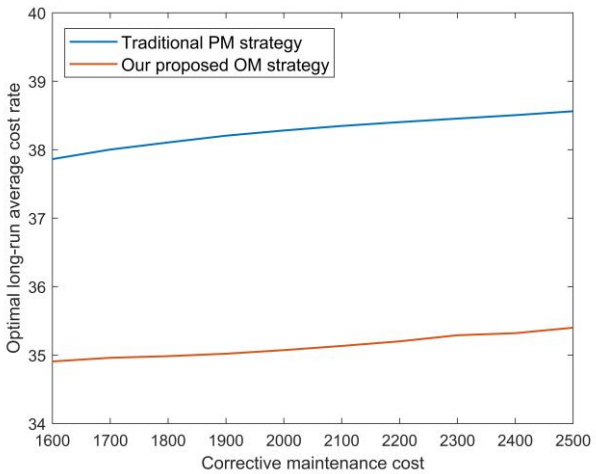

Figure 11. Sensitivity analysis on CM cost c_C.

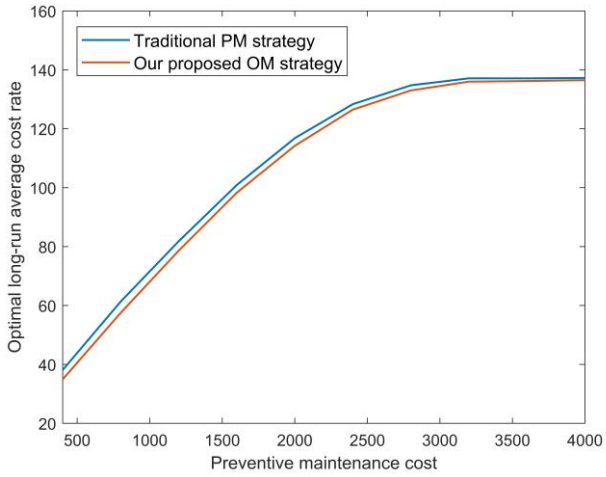

Figure 12. Sensitivity analysis on PM cost c_P.

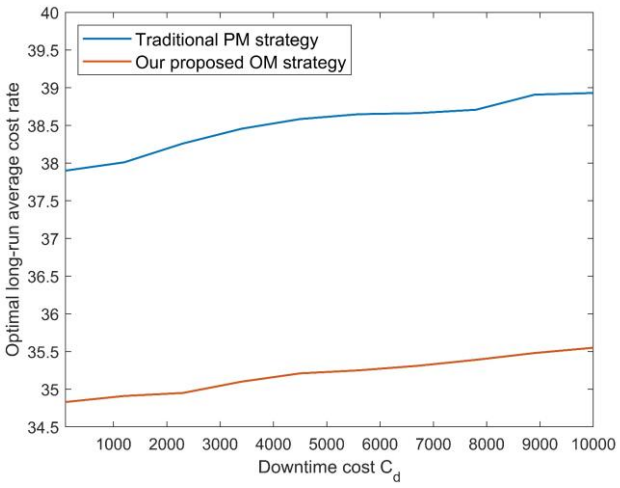

Figure 13. Sensitivity analysis on downtime cost c_d.

The above analysis is based on a popular equal load allocation policy for load-sharing systems, i.e., $\alpha_1 = \alpha_2 = 0.5$. However, due to individual heterogeneity and environmental factors, the degradation parameters of the two units are assumed to be slightly different in Table 1. Therefore, an equal load allocation policy may lead to nonnegligible individual differences between unit degradation processes, and the system reliability fails to achieve the maximum level. To address this issue, an investigation into the optimal load-sharing factor is conducted by considering the possibility of controlling and adjusting the load allocation among the two units of the novel load-sharing system.

From Figure 14, we can observe that when unit 1 is subjected to less load (0.4L) and unit 2 is subjected to more load (0.6L), the optimal long-run average cost rate of the system is minimized. This is because the degradation rate of unit 1 is slightly larger than that of unit 2. Therefore, the load-sharing factor between the two units should be adjusted so that the rapidly degrading unit 1 bears less load. Under this circumstance, the degradation processes of the two units are balanced to save substantial set-up cost caused by multiple maintenance of a single unit, and to reduce the downtime cost risk caused by the large difference in the degradation values of the two units.

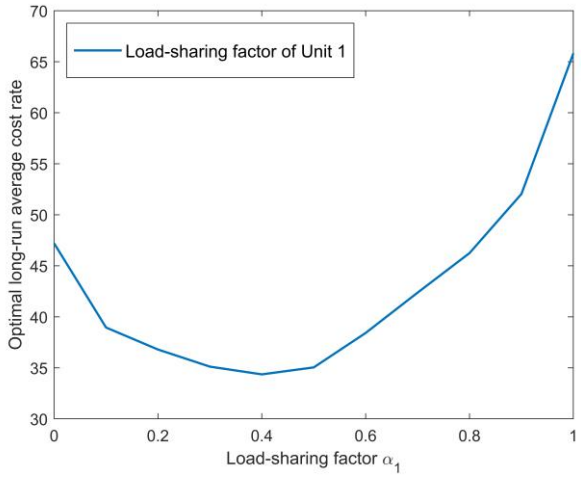

Figure 14. Investigation on the optimal load-sharing factor α_1.

4.3. Case study

To further illustrate the effectiveness and applicability of the proposed OM strategy, we conduct a case study of a two-unit GaAs laser system, where the main model parameters are referred to [13, 39-40] and listed in Table 3. It should be noted that the two laser units are degrading heterogeneously, and two parameter sets of ($a1$, $a2$, $b1$, $b2$, λ_1, λ_2) are selected as two different cases, illustrating the robustness and effectiveness of our proposed OM strategy.

Table 3. Model parameter setting of the two-unit GaAs laser system

Case	a_1	a_2	b_1	b_2	λ_1	λ_2	σ	D	L	C_S	C_P	C_C	C_I	C_d	α_1
1	0.13	0.13	1.2	1.2	0.2	0.2	0.398	10	10	5000	10000	20000	1000	40000	0.5
2	0.13	0.13	1.2	1.1	0.2	0.25	0.398								

Based on the above parameter sets, the traditional maintenance strategy and the proposed OM strategy are respectively optimized for the GaAs laser system, and the obtained minimum long-run average cost rates are presented in Table 3, along with the optimal inspection intervals and PM&OM thresholds. It is evident that our proposed OM strategy always performs better with a smaller minimum long-run cost rate, indicating robust economic benefit to perform maintenance actions on units meeting specific control limit criteria during opportunity windows created by timely maintenance on other units. These insights are inspiring for engineers involved in the maintenance decision-making of GaAs laser systems.

Table 3. Comparisons between the two strategies in two cases

Case	Maintenance strategy	Optimal inspection interval	Optimal PM threshold	Optimal OM threshold	Minimum long-run cost rate	Cost reduction
1	CBM	9.5	6.2	-	2787.1	-
	OM	9.9	7.0	4.79	2666.9	4.3%
2	CBM	10.1	4.2	-	2667.8	-
	OM	10.4	4.6	3.72	2599.6	2.6%

5. Conclusion

Motivated by a laser system example with positively correlated degradation rate and volatility, this paper presents a novel load-sharing system with a degradation rate-volatility-load correlation model, and derives the system reliability by considering the effects of unit load on both degradation rate and volatility. Furthermore, to take account of the economic dependence arising from sharable unit maintenance set-up cost, the OM strategy is introduced for the established novel load-sharing system. Based on the semi-regenerative process, the stationary distribution is obtained for the system state evolution process, and the system long-run average cost rate is derived under different scenarios, which is minimized to achieve the optimal system maintenance strategy with decision variables including inspection interval, the PM and OM threshold levels. Compared with the traditional CBM strategy separately for each unit, both an illustrative numerical example and a case study of GaAs laser system show the effectiveness and applicability of our proposed OM strategy. Besides, sensitivity analyses on representative degradation parameters and cost parameters further validate the robustness of the proposed strategy. The analysis results not only provide a valuable tool for engineers aiming to reduce maintenance expenses, but also illuminate broader managerial implications.

For future investigations of this work, the explosive investigation of the optimal load-sharing factor inspires promising research on dynamic load allocation and system operation for load-sharing systems. Another potential avenue lies in the extension of the presented novel load-sharing system to address more general degradation models and system structure.

Acknowledgments

This work is supported by National Natural Science Foundation of China (Grant: 72101170) and Sichuan Science and Technology Program (Grant: 2024NSFSC0947).

References

1. Yang C, Zeng S, Guo J. Reliability Analysis of Load-Sharing K-out-of-N System Considering Component Degradation. Mathematical Problems in Engineering 2015; 2015:1–10. http://dx.doi.org/10.1155/2015/726853
2. Zagorowska MA, Haugen T, Skourup C, Thornhill NF. Load-Sharing With Degradation Management in a Compressor Station. IEEE Transactions Automation Science and Engineering 2024; 21(1):921–938. https://doi.org/10.1109/TASE.2023.3237005.
3. Kristjanpoller F, Cárdenas-Pantoja N, Viveros P, Pascual R. Wind farm life cycle cost modelling based on oversizing capacity under load sharing configuration. Reliability Engineering & System Safety 2023; 236:109307. https://doi.org/10.1016/j.ress.2023.109307.
4. Mia S, Kumer Podder A, Manoj Kumar N, Bhatt A, Kumar K. Experimental verification of a dynamic programming and IoT-based simultaneous load-sharing controller for residential homes powered with grid and onsite solar photovoltaic electricity. Sustainable Energy

Technologies and Assessments 2023; 55:102964. https://doi.org/10.1016/j.seta.2022.102964.
5. Zhang C, Zhang Y. Common cause and load-sharing failures-based reliability analysis for parallel systems. Eksploatacja i Niezawodnosc - Maintenance and Reliability 2020; 22: 26–34. https://doi.org/10.17531/ein.2020.1.4.
6. Che H, Zeng S, Guo J. A reliability model for load-sharing k-out-of-n systems subject to soft and hard failures with dependent workload and shock effects. Eksploatacja i Niezawodnosc - Maintenance and Reliability 2020; 22: 253–264. https://doi.org/10.17531/ein.2020.2.8.
7. Wu B, Cui L. On reliability analysis of a load-sharing k -out-of- n: G system with interacting Markov subsystems. International Journal of Production Research 2022; 60: 2331–2345. https://doi.org/10.1080/00207543.2021.1887532.
8. Ye Z, Revie M, Walls L. A Load Sharing System Reliability Model With Managed Component Degradation. IEEE Transactions on Reliability 2014; 63: 721–730. https://doi.org/10.1109/ TR. 2014. 2315965.
9. Xu J, Liu B, Zhao X. Parameter estimation for load-sharing system subject to Wiener degradation process using the expectation-maximization algorithm. Quality & Reliability Engineering International 2019; 35(4): 1010–1024. https://doi.org/10.1002/qre.2442.
10. Zhao X, Liu B, Liu Y. Reliability Modeling and Analysis of Load-Sharing Systems With Continuously Degrading Components. IEEE Transactions on Reliability 2018; 67: 1096–1110. https://doi.org/10.1109/TR.2018.2846649.
11. Wu WF, Ni CC. A study of stochastic fatigue crack growth modeling through experimental data. Probabilistic Engineering Mechanics 2003; 18:107–118. https://doi.org/10.1016/S0266-8920(02)00053-X.
12. Meeker WQ, Escobar LA. Statistical methods for reliability data. New York: Wiley; 1998.
13. Ye Z-S, Chen N, Shen Y. A new class of Wiener process models for degradation analysis. Reliability Engineering & System Safety 2015; 139: 58–67. https://doi.org/10.1016/j.ress. 2015.02.005.
14. Dinh DH, Do P, Iung B, Nguyen PTN. Reliability modeling and opportunistic maintenance optimization for a multicomponent system with structural dependence. Reliability Engineering & System Safety 2024; 241: 109708. https://doi.org/10.1016/j.ress.2023.109708.
15. Shi H, Zeng J. Real-time prediction of remaining useful life and preventive opportunistic maintenance strategy for multi-component systems considering stochastic dependence. Computers & Industrial Engineering 2016; 93: 192–204. https://doi.org/10.1016/j.cie. 2015.12.016.
16. Olde Keizer MCA, Flapper SDP, Teunter RH. Condition-based maintenance policies for systems with multiple dependent components: A review. European Journal of Operational Research 2017; 261(2): 405–420. https://doi.org/10.1016/j.ejor.2017.02.044.
17. Endharta A, Ko Y. Economic Design and Maintenance of a Circular K-Out-of-n: G Balanced System With Load-Sharing Units. IEEE Transactions on Reliability 2020; 69(4): 1465–1479. https://doi.org/10.1109/TR.2020.2969236
18. Olde Keizer M, Teunter R, Veldman J, et.al. Condition-Based Maintenance for Systems with Economic Dependence and Load Sharing. International Journal of Production Economics 2018; 195: 319–327. https://doi.org/10.1016/j.ijpe.2017.10.030.
19. M. A. J. Uit Het Broek, R. H. Teunter, B. De Jonge, and J. Veldman. Joint condition-based maintenance and load-sharing optimization for two-unit systems with economic dependency. European Journal of Operational Research 2021; 295(3): 1119–1131. https://doi.org/ 10.1016/j. ejor.2021.03.044.
20. Yang X, He Y, Liao R, Cai Y, Dai W. Mission reliability-centered opportunistic maintenance approach for multistate manufacturing systems. Reliability Engineering & System Safety 2024; 241: 109693. https://doi.org/10.1016/j.ress.2023.109693.
21. Liu G, Chen S, Ho T, Ran X, Mao B, Lan Z. Optimum opportunistic maintenance schedule over variable horizons considering multi-stage degradation and dynamic strategy. Reliability Engineering & System Safety 2022; 225: 108572. https://doi.org/10.1016/j.ress.2022.108572.
22. Radner R, Jorgenson DW. Opportunistic Replacement of a Single Part in the Presence of Several Monitored Parts. Management Science 1963; 10(1): 70–84. https://doi.org/10.1287/ mnsc.10.1.70.
23. Laggoune R, Chateauneuf A, Aissani D. Impact of few failure data on the opportunistic replacement policy for multi-component systems. Reliability Engineering & System Safety 2010; 95(2): 108–119. https://doi.org/10.1016/j.ress.2009.08.007.
24. Zhang X, Zeng J. Deterioration state space partitioning method for opportunistic maintenance modelling of identical multi-unit systems. International Journal of Production Research 2015; 53(7): 2100–2118. https://doi.org/10.1080/00207543.2014.965354.
25. Vu HC, Do P, Fouladirad M, Grall A. Dynamic opportunistic maintenance planning for multi-component redundant systems with various types of opportunities. Reliability Engineering & System Safety 2020; 198: 106854. https://doi.org/10.1016/j.ress.2020.106854.
26. Xia T, Sun B, Chen Z, Pan E, Wang H, Xi L. Opportunistic maintenance policy integrating leasing profit and capacity balancing for serial-

parallel leased systems. Reliability Engineering & System Safety 2021; 205: 107233. https://doi.org/10.1016/j.ress.2020.107233.
27. Cai X, Shen J, Shen L. Reliability Evaluation and Maintenance Planning for Systems With Load-Sharing Auxiliary Components. IEEE Transactions on Reliability 2023; 72(3): 950–963. https://doi.org/10.1109/TR.2022.3215792.
28. Chelbi A, Alt-Kadi D. Analysis of a production/inventory system with randomly failing production unit submitted to regular preventive maintenance. European Journal of Operational Research 2004; 156: 712–718. https://doi.org/10.1016/S0377-2217 (03) 00254-6.
29. Kallen MJ. Modelling imperfect maintenance and the reliability of complex systems using superposed renewal processes. Reliability Engineering & System Safety 2011; 96: 636–641. https://doi.org/10.1016/j.ress.2010.12.005.
30. Keles B, Tekin S, Bakir NO. Maintenance Policies for a Deteriorating System Subject to Non-Self-Announcing Failures. IEEE Transactions on Reliability 2017; 66: 219–232. https://doi.org/10.1109/TR.2016.2639358.
31. Zhang X, Zeng J. A general modeling method for opportunistic maintenance modeling of multi-unit systems. Reliability Engineering & System Safety 2015; 140: 176–190. https://doi.org/10.1016/j.ress.2015.03.030.
32. Sun Q, Ye Z-S, Zhu X. Managing component degradation in series systems for balancing degradation through reallocation and maintenance. IISE Transactions 2020; 52: 797–810. https://doi.org/10.1080/24725854.2019.1672908.
33. Khac TH, Barros A, Berenguer C. Multi-Level Decision-Making for The Predictive Maintenance of k-Out-of-n:F Deteriorating Systems. IEEE Transactions on Reliability 2015; 64: 94–117. https://doi.org/10.1109/TR.2014.2337791.
34. Castanier B, Grall A, Bérenguer C. A condition-based maintenance policy with non-periodic inspections for a two-unit series system. Reliability Engineering & System Safety 2005; 87: 109–120. https://doi.org/10.1016/j.ress.2004.04.013.
35. Zhou Y, Zhang Z, Lin TR, Ma L. Maintenance optimisation of a multi-state series-parallel system considering economic dependence and state-dependent inspection intervals. Reliability Engineering & System Safety 2013; 111: 248–259. https://doi.org/10.1016/j.ress.2012.10.006.
36. Zhang J-X, Hu C-H, He X, Si X-S, Liu Y, Zhou D-H. A Novel Lifetime Estimation Method for Two-Phase Degrading Systems. IEEE Transactions on Reliability 2019; 68: 689–709. https://doi.org/10.1109/TR.2018.2829844.
37. Zhou X, Lu Z, Xi L. Preventive maintenance optimization for a multi-component system under changing job shop schedule. Reliability Engineering & System Safety 2012; 101: 14–20. https://doi.org/10.1016/j.ress.2012.01.005.
38. Asmussen S. Applied probability and queues. Springer Science and Business Media; 2008.
39. Peng C-Y, Tseng S-T. Mis-Specification Analysis of Linear Degradation Models. IEEE Transactions on Reliability 2009; 58: 444 – 455. https://doi.org/10.1109/TR.2009. 2026784.
40. Li Y, Shi Y, Zhang Z, Lu N, Wang X, Zio E. Condition-Based Maintenance for Performance Degradation Under Nonperiodic Unreliable Inspections. IEEE Transactions on Artificial Intelligence 2023; 4: 709 – 721. https://doi.org/10.1109/TAI. 2022.3197680.

Appendix A

A.1. Proof of Equation (9)

The analytical result of Equation (9) is derived as follows:

$$f_{(1)T_2}(s)=\int_{-\infty}^{D_2} f_{(1)T_2}(s|x_{2,\tau})\,g(x_{2,\tau})dx_{2,\tau}=\int_{-\infty}^{D}\frac{D_2-x_{2,\tau}}{\sqrt{2\pi\sigma_{2,2}^2(s-\tau)^3}}exp\left\{-\frac{\left(D_2-x_{2,\tau}-\mu_{2,2}(s-\tau)\right)^2}{2\sigma_{2,2}^2(s-\tau)}\right\}$$

$$\times\frac{1}{\sqrt{2\pi\tau[\vartheta_2(\varphi_2(L_2))]^2}}\left\{exp\left[-\frac{\left(x_{2,\tau}-\varphi_2(L_2)\tau\right)^2}{2[\vartheta_2(\varphi_2(L_2))]^2\tau}\right]-exp\left[\frac{2D_2\varphi_2(L_2)}{[\vartheta_2(\varphi_2(L_2))]^2}\right]exp\left[-\frac{\left(x_{2,\tau}-2D_2-\varphi_2(L_2)\tau\right)^2}{2[\vartheta_2(\varphi_2(L_2))]^2\tau}\right]\right\}dx_{2,\tau}$$

$$=\int_{-\infty}^{D_2}\frac{D_2-x_{2,\tau}}{2\pi\vartheta_2(\varphi_2(L_2))\sigma_{2,2}\sqrt{(s-\tau)^3\tau}}\left\{exp\left[-\frac{\left(D_2-x_{2,\tau}-\mu_{2,2}(s-\tau)\right)^2}{2\sigma_{2,2}^2(s-\tau)}-\frac{\left(x_{2,\tau}-\varphi_2(L_2)\tau\right)^2}{2[\vartheta_2(\varphi_2(L_2))]^2\tau}\right]\right.$$

$$\left.-exp\left[\frac{2D_2\varphi_2(L_2)}{[\vartheta_2(\varphi_2(L_2))]^2}\right]\cdot exp\left[-\frac{\left(D_1-x_{2,\tau}-\mu_{2,2}(s-\tau)\right)^2}{2\sigma_{2,2}^2(s-\tau)}-\frac{\left(x_{2,\tau}-2D_2-\varphi_2(L_2)\tau\right)^2}{2[\vartheta_2(\varphi_2(L_2))]^2\tau}\right]\right\}dx_{2,\tau}=\text{Int1}-\text{Int2} \quad (24)$$

where the first segment on the right side is described as Int1 and derived by:

$$\text{Int1} = \int_{-\infty}^{D_2} \frac{D_2 - x_{2,\tau}}{2\pi\vartheta_2(\varphi_2(L_2))\sigma_{2,2}\sqrt{(s-\tau)^3\tau}} \cdot exp\left\{ - \frac{\left[x_{2,\tau} - \frac{\tau}{\tau[\vartheta_2(\varphi_2(L_2))]^2 + (s-\tau)\sigma_{2,2}^2}\left(D_2[\vartheta_2(\varphi_2(L_2))]^2 + (s-\tau)(\sigma_{2,2}^2\varphi_2(L_2) - [\vartheta_2(\varphi_2(L_2))]^2\mu_{2,2})\right)\right]^2}{\frac{2[\vartheta_2(\varphi_2(L_2))]^2\sigma_{2,2}^2(s-\tau)\tau}{\tau[\vartheta_2(\varphi_2(L_2))]^2 + (s-\tau)\sigma_{2,2}^2}} \right.$$

$$+ \frac{\sigma_{2,1}^2 D_2\tau + (s\tau - \tau^2)(\sigma_{2,2}^2\varphi_2(L_2) - [\vartheta_2(\varphi_2(L_2))]^2\mu_{2,2})}{2[\vartheta_2(\varphi_2(L_2))]^4\sigma_{2,2}^2(s-\tau)\tau^2 + 2[\vartheta_2(\varphi_2(L_2))]^2\sigma_{2,2}^4(s-\tau)^2\tau}$$

$$\left. - \frac{\left(\tau[\vartheta_2(\varphi_2(L_2))]^2 + (s-\tau)\sigma_{2,2}^2\right)\left([\vartheta_2(\varphi_2(L_2))]^2\tau\left(D_2 - \mu_{2,2}(s-\tau)\right)^2 + (s-\tau)\sigma_{2,2}^2\varphi_2^2(L_2)\tau^2\right)}{2[\vartheta_2(\varphi_2(L_2))]^4\sigma_{2,2}^2(s-\tau)\tau^2 + 2[\vartheta_2(\varphi_2(L_2))]^2\sigma_{2,2}^4(s-\tau)^2\tau} \right\} dx_{2,\tau} \tag{25}$$

$$= \int_{-\infty}^{D_2} \left\{ \frac{exp(A)D_2}{2\pi\vartheta_2(\varphi_2(L_2))\sigma_{2,2}\sqrt{(s-\tau)^3\tau}} \right.$$

$$\cdot exp\left\{ - \frac{\left[x_{2,\tau} - \frac{\tau}{\tau[\vartheta_2(\varphi_2(L_2))]^2 + (s-\tau)\sigma_{2,2}^2}\left(D_2[\vartheta_2(\varphi_2(L_2))]^2 + (s-\tau)(\sigma_{2,2}^2\varphi_2(L_2) - [\vartheta_2(\varphi_2(L_2))]^2\mu_{2,2})\right)\right]^2}{\frac{2[\vartheta_2(\varphi_2(L_2))]^2\sigma_{2,2}^2(s-\tau)\tau}{\tau[\vartheta_2(\varphi_2(L_2))]^2 + (s-\tau)\sigma_{2,2}^2}} \right\}$$

$$\left. - \frac{exp(A)x_{2,\tau}}{2\pi\vartheta_2(\varphi_2(L_2))\sigma_{2,2}\sqrt{(s-\tau)^3\tau}} \cdot exp\left\{ - \frac{\left[x_{2,\tau} - \frac{\tau}{\tau[\vartheta_2(\varphi_2(L_2))]^2 + (s-\tau)\sigma_{2,2}^2}\left(D_2[\vartheta_2(\varphi_2(L_2))]^2 + (s-\tau)(\sigma_{2,2}^2\varphi_2(L_2) - [\vartheta_2(\varphi_2(L_2))]^2\mu_{2,2})\right)\right]^2}{\frac{2[\vartheta_2(\varphi_2(L_2))]^2\sigma_{2,2}^2(s-\tau)\tau}{\tau[\vartheta_2(\varphi_2(L_2))]^2 + (s-\tau)\sigma_{2,2}^2}} \right\} \right\} dx_{2,}$$

$$= \frac{exp(A)D_2}{\sqrt{[\vartheta_2(\varphi_2(L_2))]^2\pi(s-\tau)^2\tau + \sigma_{2,2}^2\pi(s-\tau)^3}} \cdot \Phi\left[\frac{D_2 - \frac{\tau}{\tau[\vartheta_2(\varphi_2(L_2))]^2 + (s-\tau)\sigma_{2,2}^2}\left(D_2[\vartheta_2(\varphi_2(L_2))]^2 + (s-\tau)(\sigma_{2,2}^2\varphi_2(L_2) - [\vartheta_2(\varphi_2(L_2))]^2\mu_{2,2})\right)}{\sqrt{\frac{2[\vartheta_2(\varphi_2(L_2))]^2\sigma_{2,2}^2(s-\tau)\tau}{\tau[\vartheta_2(\varphi_2(L_2))]^2 + (s-\tau)\sigma_{2,2}^2}}} \right] + \frac{exp(A)}{2\pi\vartheta_2(\varphi_2(L_2))\sigma_{2,2}\sqrt{(s-\tau)^3\tau}} \cdot$$

$$exp\left[- \frac{\left[D_2 - \frac{\tau}{\tau[\vartheta_2(\varphi_2(L_2))]^2 + (s-\tau)\sigma_{2,2}^2}\left(D_2[\vartheta_2(\varphi_2(L_2))]^2 + (s-\tau)(\sigma_{2,2}^2\varphi_2(L_2) - [\vartheta_2(\varphi_2(L_2))]^2\mu_{2,2})\right)\right]^2}{\frac{2[\vartheta_2(\varphi_2(L_2))]^2\sigma_{2,2}^2(s-\tau)\tau}{\tau[\vartheta_2(\varphi_2(L_2))]^2 + (s-\tau)\sigma_{2,2}^2}} \right]$$

and the second segment on the right side is described as Int2 and derived by:

$$\text{Int2} = \int_{-\infty}^{D_2} exp\left(\frac{2D_2\varphi_2(L_2)}{[\vartheta_2(\varphi_2(L_2))]^2}\right) \frac{D_2 - x_{2,\tau}}{2\pi\vartheta_2(\varphi_2(L_2))\sigma_{2,2}\sqrt{(s-\tau)^3\tau}} \cdot exp\left[- \frac{\left(D_2 - x_{2,\tau} - \mu_{2,2}(s-\tau)\right)^2}{2\sigma_{2,2}^2(s-\tau)} - \frac{\left(x_{2,\tau} - 2D_2 - \varphi_2(L_2)\tau\right)^2}{2[\vartheta_2(\varphi_2(L_2))]^2\tau} \right] dx_{2,\tau}$$

$$= \int_{-\infty}^{D_2} exp\left[\frac{2D_2\varphi_2(L_2)}{[\vartheta_2(\varphi_2(L_2))]^2}\right] \frac{D_2 - x_{2,\tau}}{2\pi\vartheta_2(\varphi_2(L_2))\sigma_{2,2}\sqrt{(s-\tau)^3\tau}} \cdot exp\left\{ - \frac{\left[x_{2,\tau} - \frac{\left(\tau[\vartheta_2(\varphi_2(L_2))]^2\left(D_2 - \mu_{2,2}(s-\tau)\right) + (s-\tau)\sigma_{2,2}^2(2D_2 + \varphi_2(L_2)\tau)\right)}{\tau[\vartheta_2(\varphi_2(L_2))]^2 + (s-\tau)\sigma_{2,2}^2}\right]^2}{\frac{2[\vartheta_2(\varphi_2(L_2))]^2\sigma_{2,2}^2(s-\tau)\tau}{\tau[\vartheta_2(\varphi_2(L_2))]^2 + (s-\tau)\sigma_{2,2}^2}} \right.$$

$$- \frac{\left(\tau[\vartheta_2(\varphi_2(L_2))]^2 + (s-\tau)\sigma_{2,2}^2\right)\left[\tau[\vartheta_2(\varphi_2(L_2))]^2\left(D_2 - \mu_{2,2}(s-\tau)\right)^2 + (s-\tau)\sigma_{2,2}^2(2D_2 + \varphi_2(L_2)\tau)^2\right]}{2[\vartheta_2(\varphi_2(L_2))]^4\sigma_{2,2}^2(s-\tau)\tau^2 + 2[\vartheta_2(\varphi_2(L_2))]^2\sigma_{2,2}^4(s-\tau)^2\tau}$$

$$\left. + \frac{\left(\tau[\vartheta_2(\varphi_2(L_2))]^2\left(D_2 - \mu_{2,2}(s-\tau)\right) + (s-\tau)\sigma_{2,2}^2(2D_2 + \varphi_2(L_2)\tau)\right)^2}{2[\vartheta_2(\varphi_2(L_2))]^4\sigma_{2,2}^2(s-\tau)\tau^2 + 2[\vartheta_2(\varphi_2(L_2))]^2\sigma_{2,2}^4(s-\tau)^2\tau} \right\} dx_{2,\tau}$$

$$= \int_{-\infty}^{D_2} \left\{ \frac{exp\left[\frac{2D_2\varphi_2(L_2)}{[\vartheta_2(\varphi_2(L_2))]^2} + B\right] D_2}{2\pi\vartheta_2(\varphi_2(L_2))\sigma_{2,2}\sqrt{(s-\tau)^3\tau}} exp\left\{ - \frac{\left[x_{2,\tau} - \frac{\left(\tau[\vartheta_2(\varphi_2(L_2))]^2\left(D_2 - \mu_{2,2}(s-\tau)\right) + (s-\tau)\sigma_{2,2}^2(2D_2 + \varphi_2(L_2)\tau)\right)}{\tau[\vartheta_2(\varphi_2(L_2))]^2 + (s-\tau)\sigma_{2,2}^2}\right]^2}{\frac{2[\vartheta_2(\varphi_2(L_2))]^2\sigma_{2,2}^2(s-\tau)\tau}{\tau[\vartheta_2(\varphi_2(L_2))]^2 + (s-\tau)\sigma_{2,2}^2}} \right\} \right.$$

$$\left. - \frac{exp\left[\frac{2D_2\varphi_2(L_2)}{\sigma_2^2} + B\right] x_{2,\tau}}{2\pi\vartheta_2(\varphi_2(L_2))\sigma_{2,2}\sqrt{(s-\tau)^3\tau}} exp\left\{ - \frac{\left[x_{2,\tau} - \frac{\left(\tau[\vartheta_2(\varphi_2(L_2))]^2\left(D_2 - \mu_{2,2}(s-\tau)\right) + (s-\tau)\sigma_{2,2}^2(2D_2 + \varphi_2(L_2)\tau)\right)}{\tau[\vartheta_2(\varphi_2(L_2))]^2 + (s-\tau)\sigma_{2,2}^2}\right]^2}{\frac{2[\vartheta_2(\varphi_2(L_2))]^2\sigma_{2,2}^2(s-\tau)\tau}{\tau[\vartheta_2(\varphi_2(L_2))]^2 + (s-\tau)\sigma_{2,2}^2}} \right\} \right\} dx_{2,\tau}$$

$$= \frac{exp\left[\frac{2D_2\varphi_2(L_2)}{[\vartheta_2(\varphi_2(L_2))]^2} + B\right] D_2}{\sqrt{[\vartheta_2(\varphi_2(L_2))]^2\pi(s-\tau)^2\tau + \sigma_{2,2}^2\pi(s-\tau)^3}} \Phi\left[\frac{D_2 - \frac{\left(\tau[\vartheta_2(\varphi_2(L_2))]^2\left(D_2 - \mu_{2,2}(s-\tau)\right) + (s-\tau)\sigma_{2,2}^2(2D_2 + \varphi_2(L_2)\tau)\right)}{\tau[\vartheta_2(\varphi_2(L_2))]^2 + (s-\tau)\sigma_{2,2}^2}}{\sqrt{\frac{2[\vartheta_2(\varphi_2(L_2))]^2\sigma_{2,2}^2(s-\tau)\tau}{\tau[\vartheta_2(\varphi_2(L_2))]^2 + (s-\tau)\sigma_{2,2}^2}}}\right]$$

$$+ \frac{exp\left[\frac{2D_2\varphi_2(L_2)}{\sigma_2^2} + B\right]}{2\pi\vartheta_2(\varphi_2(L_2))\sigma_{2,2}\sqrt{(s-\tau)^3\tau}} exp\left\{-\frac{\left[D_2 - \frac{\left(\tau[\vartheta_2(\varphi_2(L_2))]^2(D_2 - \mu_{2,2}(s-\tau)) + (s-\tau)\sigma_{2,2}^2(2D_2 + \varphi_2(L_2)\tau)\right)}{\tau[\vartheta_2(\varphi_2(L_2))]^2 + (s-\tau)\sigma_{2,2}^2}\right]^2}{\frac{2[\vartheta_2(\varphi_2(L_2))]^2\sigma_{2,2}^2(s-\tau)\tau}{\tau[\vartheta_2(\varphi_2(L_2))]^2 + (s-\tau)\sigma_{2,2}^2}}\right\} \quad (26)$$

Where:

$$A = \frac{[\vartheta_2(\varphi_2(L_2))]^2 D_2\tau + (s\tau - \tau^2)(\sigma_{2,2}^2\varphi_2(L_2) - [\vartheta_2(\varphi_2(L_2))]^2\mu_{2,2})}{2[\vartheta_2(\varphi_2(L_2))]^4\sigma_{2,2}^2(s-\tau)\tau^2 + 2[\vartheta_2(\varphi_2(L_2))]^2\sigma_{2,2}^4(s-\tau)^2\tau}$$

$$- \frac{\left(\tau[\vartheta_2(\varphi_2(L_2))]^2 + (s-\tau)\sigma_{2,2}^2\right)\left([\vartheta_2(\varphi_2(L_2))]^2\tau\left(D_2 - \mu_{2,2}(s-\tau)\right)^2 + (s-\tau)\sigma_{2,2}^2[\vartheta_2(\varphi_2(L_2))]^2\tau^2\right)}{2[\vartheta_2(\varphi_2(L_2))]^4\sigma_{2,2}^2(s-\tau)\tau^2 + 2[\vartheta_2(\varphi_2(L_2))]^2\sigma_{2,2}^4(s-\tau)^2\tau}$$

$$B = -\frac{\left(\tau[\vartheta_2(\varphi_2(L_2))]^2 + (s-\tau)\sigma_{2,2}^2\right)\left[\tau[\vartheta_2(\varphi_2(L_2))]^2\left(D_2 - \mu_{2,2}(s-\tau)\right)^2 + (s-\tau)\sigma_{2,2}^2(2D_2 + \varphi_2(L_2)\tau)^2\right]}{2[\vartheta_2(\varphi_2(L_2))]^4\sigma_{2,2}^2(s-\tau)\tau^2 + 2[\vartheta_2(\varphi_2(L_2))]^2\sigma_{2,2}^4(s-\tau)^2\tau}$$

$$+ \frac{\left(\tau[\vartheta_2(\varphi_2(L_2))]^2\left(D_2 - \mu_{2,2}(s-\tau)\right) + (s-\tau)\sigma_{2,2}^2(2D_2 + \varphi_2(L_2)\tau)\right)^2}{2[\vartheta_2(\varphi_2(L_2))]^4\sigma_{2,2}^2(s-\tau)\tau^2 + 2[\vartheta_2(\varphi_2(L_2))]^2\sigma_{2,2}^4(s-\tau)^2\tau}$$

A.2. Proof of Lemma 1

A discrete Markov chain $\{X_i(t_k), k = 1, 2, \ldots, N; i = 1,2\}$ on a general space Ω is Harris recurrent if and only if it has a regeneration set [38]. Consider $B(\Omega)$ as the Borel set of the state space Ω. On the basis of Asmussen [38, Chapter VII.3], a set $U \in B(\Omega)$ is a regeneration set if there exists some $\epsilon \in (0,1), r > 0$, and a probability measure F, such that

For some $k \geq 1, \forall\, x \in \Omega, \mathrm{P}(\, X_i(t_k) \in U \mid X_i(t_0) = x\,) = 1$;

If $x_i \in U$ and $C \subseteq B(\Omega)$, then $P(\, X_i(t_r) \in C \mid X_i(t_0) = x_i\,) \geq \epsilon\mathcal{F}(C)$.

In this study, a set $U \equiv \{(x_1, x_2) \in \Omega | x \geq M_p, x_2 \geq M_o\} \cup \{(x_1, x_2) \in \Omega | x_1 \geq M_o, x_2 \geq M_p\}$ is constructed to be the set of two-unit states that both units will be maintained simultaneously at an inspection epoch. It is worth noting that if the degenerate states of both units belong to U, then they will be replaced and the system will also return to the initial state with probability 1 in a finite amount of time, regardless of the initial state. In other words, the first condition holds. At the same time, the degraded state of two units in the system during the next inspection cycle is not affected by the historical state if both components are replaced at the current maintenance time. In other words, if the condition x ∈ U is met, then:

$$P(\, X_i(t_1) \in C \mid X_i(t_0) = x_i\,) = P(\, X_i(t_1) \in C \mid X_i(t_0) = 0\,) \quad (27)$$

For all $C \subseteq B(\Omega)$. Set $r = 1$ and $\mathcal{F}(\mathrm{C}) = P(\, X_i(t_1) \in C \mid X_i(t_0) = 0\,)$, the second condition to guarantee that U is a regeneration set is satisfied for any $\epsilon \in (0,1)$ on the basis of (24). Therefore, we can conclude that the embedded Markov chain $\{X_i(t_k), k = 1, 2, \ldots, N; i = 1,2\}$ is a Harris recurrent and the stationary distribution π exists. Consider $\pi(y_1, y_2)$ as the stationary probability distribution function of two units in a load-sharing system for $y_i \in (-\infty, +\infty)$. Then, the following formula:

$$\int_{-\infty}^{+\infty}\int_{-\infty}^{+\infty} \pi(y_1, y_2)\, dy_1 dy_2 = 1 \quad (28)$$

is met.